Chapter 13

Review of In Vitro Toxicity of Nanoparticles and Nanorods—Part 2

Jose E. Perez, Nouf Alsharif, Aldo I. Martínez-Banderas, Basmah Othman, Jasmeen Merzaban, Timothy Ravasi and Jürgen Kosel

Additional information is available at the end of the chapter

http://dx.doi.org/10.5772/intechopen.78616

Abstract

The specific use of engineered nanostructures in biomedical applications has become very attractive, due to their ability to interface and target specific cells and tissues to execute their functions. Additionally, there is continuous progress in research on new nanostructures with unique optical, magnetic, catalytic and electrochemical properties that can be exploited for therapeutic or diagnostic methods. On the other hand, as nanostructures become widely used in many different applications, the unspecific exposure of humans to them is also unavoidable. Therefore, studying and understanding the toxicity of such materials are of increasing importance. Previously published reviews regarding the toxicological effects of nanostructures focus mostly on the cytotoxicity of nanoparticles and their internalization, activated signaling pathways and cellular response. Here, the most recent studies on the in-vitro cytotoxicity of NPs, nanowires and nanorods for biomedical applications are reviewed and divided into two parts. The first part considers nonmagnetic metallic and magnetic nanostructures, while, the second part covers carbon structures and semiconductors. The factors influencing the toxicity of these nanostructures are elaborated to help elucidate the effects of these nanomaterials on cells, which is a prerequisite for their safe clinical use.

Keywords: nanoparticles, nanowires, nanorods, biocompatibility, cytotoxicity, nanomedicine

1. Introduction

Nanostructured materials are defined as possessing one of their dimensions ranging from 1 to 100 nm, according to the American Society for Testing and Materials (ASTM) international standards definition [1]. For nanoparticles (NPs), which can be of more or less spherical or cubical shape, two dimensions are required to be within this range. In contrast, the shape of nanorods (NRs) is in one dimension much larger than in the others. For a small aspect ratio (<10) both their length and diameter are in the nanoscale, whereas NRs with a large aspect ratio (>10) only have their diameter within this scale, and they are often called "nanowires" (NWs). Nanostructures within this specific size scale show unique size-dependent optical, magnetic, catalytic and electrochemical properties, among others, as well as high surface to volume ratios. Moreover, their shape, surface chemistry and chemical composition can be used to tailor-specific properties, making nanostructures highly versatile for different applications [2, 3].

The size scale of nanostructures is within the range of several biomolecules, such as proteins and antibodies, allowing specific interactions to occur between them. This, when coupled with the high surface to volume ratios and tunable sizes and properties, makes nanostructures prime candidates for biomedical applications such as imaging, drug delivery and therapy [4–6]. Examples of applications include the use of NPs as magnetic resonance imaging (MRI) contrast agents [7, 8], tissue engineering [9–11], as well as the recent focus on hyperthermia and cancer cell eradication with the use of NPs and NRs [12–17]. Such applications, if they are aimed for a clinical setting, ultimately require a direct NP/NR exposure in the form of ingestion or intravenous delivery into the body. Naturally, there is a rigorous testing required before any new drug formulation is approved for clinical use in order to ensure their safety and effectiveness. Currently, very few NPs-based drugs have been approved by the Food and Drug Administration and are commercially available. Examples include GastroMARK, used as an MRI contrast agent to enhance the delineation of the bowel, and ferumoxytol, an iron-replacement formulation approved for adults with chronic kidney disease with an iron deficiency [18].

Within this scope, biocompatibility and cytotoxicity data are of paramount importance to evaluate the potential of nanostructures for biomedical applications. Nanostructures are normally engineered to interface and target-specific cells or tissues to execute their functions, raising questions about their toxicological effects. For instance, there are several characteristics involved in the toxicity of fiber-like nanomaterials, such as shape, length, chemical composition, agglomeration and purity, making them suitable to fit the "fiber toxicological paradigm" according to the World Health Organization (WHO) criteria used to describe the toxicity of asbestos fibers [19]. Further, nanostructures are usually tuned for biocompatibility on top of the desired biomedical function, with the most relevant aspects that influence their toxicity being the material [20], size and shape [21], surface charge [22] and surface functionalization [23]. In vitro studies, while not able to give a complete insight into the biocompatibility of nanostructures, have a high importance, due to their easy implementation, and provide valuable cytotoxicology data regarding the safety of the use of nanostructures in biomedical applications. Previously published reviews regarding the biosafety of nanostructures include that of Lewinski et al. [24] and Zhao et al. [25]. The former focuses mostly on the cytotoxicity of

http://dx.doi.org/10.5772/intechopen.78616

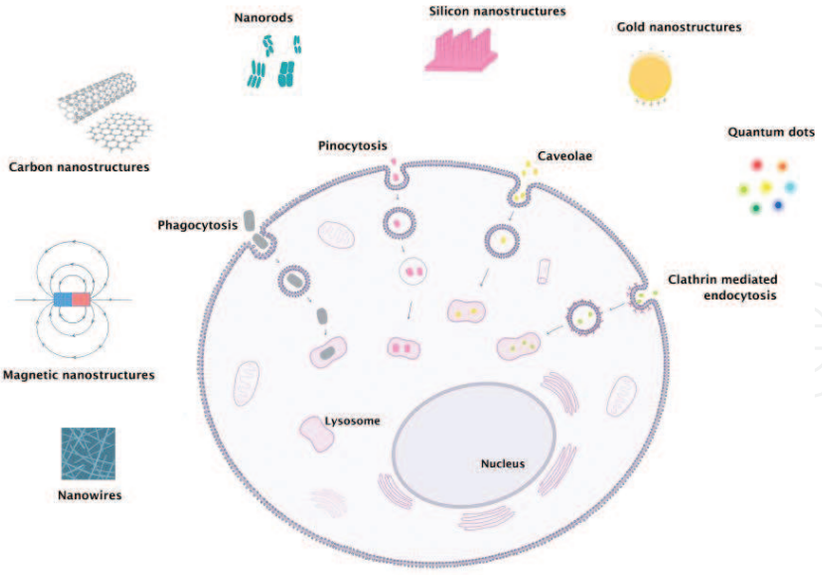

Figure 1. Schematic of the pathways for intracellular uptake of different materials and structures.

NPs of different materials, as well as carbon nanotubes (CNTs), whereas the latter is a more in-depth review of the internalization, activated signaling pathways and cellular response of different kinds of NPs.

Here, we review relevant studies assessing the *in vitro* cytotoxicity of both nanoparticles (NPs) and nanowires (NWs)/nanorods (NRs) with the potential to be used in biomedical applications. Due to their prevalence within the applied nanomaterials in biomedicine, this chapter covers various materials from four different classes (on Scopus almost 50% of all publications related to cytotoxicity, since the year 2000, fall within these materials) that are typically considered in the context of nanomaterials for biomedical applications. The first part of this chapter covers nonmagnetic metals and magnetic materials, while the second part covers carbon structures and semiconductors. An overview of the materials and structures covered, together with the various intracellular uptake mechanisms, is given in **Figure 1**.

2. Carbon nanostructures

Carbon nanostructures include a broad diversity of carbon allotropes that differ from pristine diamond and graphite. Carbon has been used in many technological applications, exploiting its capability of forming networks composed exclusively of C-atoms with the same electronic configuration or hybridizing configurations sp^3-, sp^2- and sp-, expanding the possible allotropes that can be constructed [26]. Since the synthesis of the first carbon nanostructures, such as fullerene C_{60} (0D) [27] and CNTs (1D) [28] (**Figure 2**), there has been a tremendous effort for understanding the properties of these nanomaterials and for exploring the broad range of applications in which they can be used. Carbon-based nanomaterials (CNMs) have created a great deal of interest in various applications such as optical imaging [29], drug and gene delivery [30], and nanotherapeutics [31, 32] due to their excellent mechanical, optical and electrical

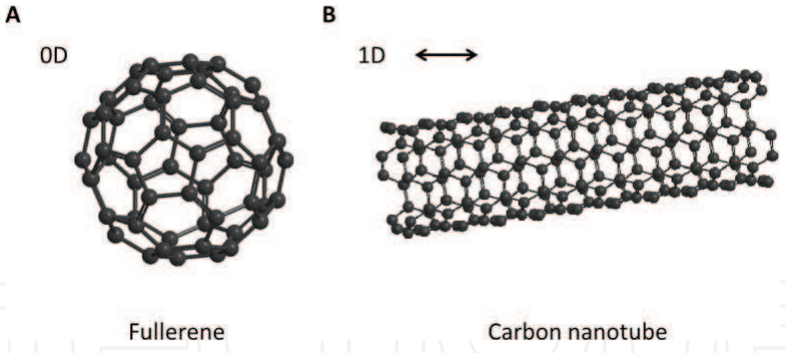

Figure 2. Chemical structure of representative carbon-based nanomaterials. Structure of fullerene C_{60} (A) and carbon nanotube (B).

properties [33–35], as well as due to their ability to translocate through the cell membrane or be internalized via energy-dependent endocytic pathways [36]. Similarly, CNMs possess an extraordinary ability to be loaded with drugs or different chemical agents that are either attached to the surface or, in the case of CNTs, they can be packed into the interior cores [37].

These widespread applications of CNMs are also accompanied by increasing concerns regarding their interactions with tissues, cells, and biomolecules as well as degradation pathways, and at a macroscale, the potential deleterious effects on human health and the environment.

2.1. Fullerene C_{60}

The structure of fullerene C_{60}, which has a van der Walls diameter of approximately 1 nm, is formed from 60 carbon atoms arranged in a spherical, cage-like structure consisting of 60 vertices, 12 pentagonal faces and 20 hexagonal faces [38]. Fullerenes and their derivatives are probably the most extensively studied NPs with several properties and applications including MRI [39], drug delivery [40, 41], photodynamic therapy (PDT) [40] and photothermal therapy (PTT) [42].

Although fullerenes are generally hydrophobic molecules, many strategies have been developed for improving their solubilization in water that is, synthesized water-soluble derivatives of fullerenes by chemical modifications through the addition of functional groups such as hydroxyl-, carboxyl-, amino- and alkyl-groups and other side-chain/cyclic moieties to the C_{60} structure [43]. The different methods employed to increase C_{60} water solubility profoundly influence the physiochemical properties and the toxicological effects of these compounds, raising uncertainties about the possible consequences on human health and potential medical uses [44]. Nakagawa et al. studied the effects of the hydroxylated fullerenes (fullerenols) $C_{60}(OH)_{24}$ and $C_{60}(OH)_{12}$ 0.125 mM in rat hepatocytes, observing a concentration and time-dependent cell death accompanied by mitochondrial dysfunction, with $C_{60}(OH)_{24}$ found to be more cytotoxic with almost 100% of cell death after 30 min. The authors concluded that the toxic effects of fullerenols may depend on the number of hydroxyl groups [38]. $C_{60}(OH)_{24}$ at a concentration of 0.1 mM caused cell blebbing, loss of cellular ATP and lipid peroxidation in rat hepatocytes [45]. Similarly, the cytotoxic effects of fullerene C_{60} and the derivatives $C_{60}(OH)_2$, $C_{60}(OH)_{6–12}$, $C_{60}(OH)_{12}$ and $C_{60}(OH)_{36}$, were evaluated in three different types of liver cells:

http://dx.doi.org/10.5772/intechopen.78616

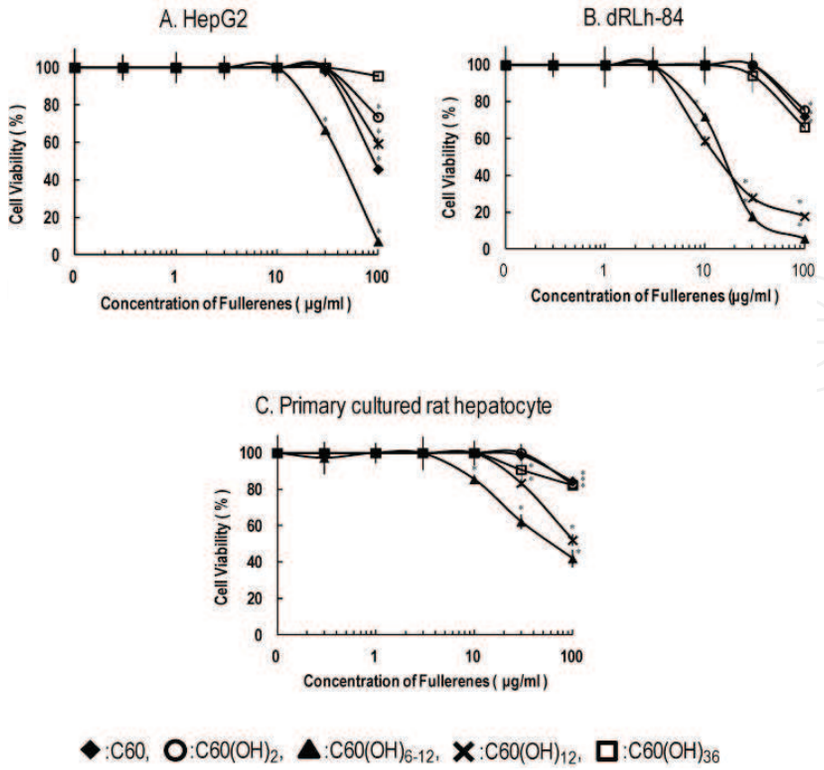

Figure 3. Cytotoxicity of fullerene and hydroxylated fullerenes in liver cells. HepG2 (A); dRLh-84 (B); and primary cultured rat hepatocytes (C) were exposed to C60, C60(OH)2, C60(OH)6–12, C60(OH)12 and C60(OH)36 for 3 days. Data are represented as mean ± SD (n = 3). (*) statistically significant from control ($p < 0.05$). Adapted from Shimizu et al. [46]. Copyright 2013 by the authors. Licensee MDPI, Basel, Switzerland. CC BY 3.0.

dRLh-84, HepG2 and rat hepatocytes as shown in **Figure 3** [46]. $C_{60}(OH)_{6–12}$ and $C_{60}(OH)_{12}$ were found to induce cytotoxic effects after 3 days of exposure in dRLh-84 cells at a concentration of 10 μg/mL reducing the cell viability 30 and 40%, respectively, in the form of inhibition of mitochondrial activity. Similarly, to Nakawaga's findings, these results indicate that the number of hydroxyl groups on $C_{60}(OH)_x$ contributes to the cytotoxic potential and mitochondrial damage.

Other fullerene derivatives have also been tested for cytotoxic effects in human epithelial HEp-2 cells, such as C_{60}-PVP, C_{60}-NO_2-proline and sodium salt of polycarboxylic C_{60} [47]. However, the PVP and NO_2-proline derivatives did not have an effect on cell viability, and the sodium salt of polycarboxylic derivative induced a drastic decrease in cell number of about 80% at a concentration around 0.1 mg/mL.

Further, the molecular mechanisms underlying the cytotoxic effects of two similar fullerene derivatives (C_{60}-1,3-dipolar cycloaddition of azomethine ylides) on human MCF-7 cells were analyzed by RNA-seq-based gene expression [44]. It was found that whereas one derivative had a negligible effect, the addition of an extra trifluoroacetate group induced a significant, time-dependent alteration of gene expression, mainly in biological processes involving protein synthesis, cell cycle progression and cell adhesion, with the authors suggesting an inhibition effect of the mTOR pathway.

In a recent study performed by Canape et al., C_{60} fullerenes were covalently functionalized with PEG of various sizes, Full–PEG2000, Full–PEG5000 and Full–PEG10000, and viability was studied on a variety of cell lines 24 h after exposure, evaluating mitochondrial activity, cell membrane integrity and hemolysis [48]. However, all the tested compounds were found to reduce, to some extent, the cellular metabolic activity, only two affected the cell membrane integrity, and none induced hemolysis. It was concluded that fullerenes C_{60} functionalized with higher molecular weight PEGs possess a higher biocompatibility and that side toxicity can be alleviated using proper surface coating. Together, all these findings support that the surface functionalization of fullerenes plays an important role with regard to their interaction with biological systems.

The interaction of CNMs with lipid membranes is of great interest because biological activity requires crossing or breaking lipid membranes. In a study concerning the interaction of fullerenes with the lipid bilayer and the possibility of fullerene crossing it, it was observed that hydrophobic molecules of C_{60} were localized within the inner part of the membrane, whereas hydrophilic C_{60}(OH)n fullerenols molecules were adsorbed on the heads of membrane phospholipids [49], where they can interact with membrane proteins, such as ATPases and influence their activity [50, 51]. Similarly, Raoof et al. showed that the internalization of a water-soluble derivatized C_{60} malonodiserinolamide takes place through multiple energy-dependent pathways, and they escape endocytotic vesicles to eventually localize and accumulate in the nucleus through the nuclear pore complex [41].

2.2. Single-walled carbon nanotubes

CNTs are classified in single-walled carbon nanotubes (SWCNTs) and multiwalled carbon nanotubes (MWCNTs). The first ones are formed from a single layer of graphene (0.4–10 nm in diameter), whereas the second ones consist of multiple concentric cylinders of graphene with increasing diameters (10–100 nm) [52]. The length of CNTs can range from nanometers to centimeters [53], and they possess unique physical and chemical properties such as a lightweight, high tensile strength, high electrical and thermal conductivities, unique optical properties and extreme chemical stability, as well as high surface-to-volume ratios with reactive surface chemistries. Such properties have made CNTs an interesting material for biomedical applications, where they have been used as drug, protein and nucleic acid delivery tools [54–56], cancer cell destruction [57, 64, 91], diagnostics [59] and as noninvasive and highly sensitive imaging aids [31, 58]. Naturally, biosafety concerns of CNTs are rapidly emerging with numerous reports indicating their potential hazards to the public health.

The graphene sheets can be wrapped in a variety of ways that are denoted by a pair of indices (n, m), which define both the diameter and the chirality of SWCNTs, which can be either metallic (M) or semiconducting (S). As synthesized, SWNTs have a wide range of diameters and chiral angles, which leads to a polydisperse sample of discrete properties [59, 60]. SWCNTs possess small diameters and the large aspect ratios that render them ideal one-dimensional quantum wires that elicit different biological behavior compared to spherical NPs, when introduced in biological systems [26]. The cytotoxicity of pristine SWCNTs and

SWCNTs functionalized with PEG has been evaluated with neuronal PC12 cells at the biochemical, cellular and gene expression levels by Zhang et al. [61]. Cytotoxicity increased with the concentration, whereby SWCNT-PEGs exhibited less cytotoxic potency than bare SWCNTs at the highest concentration tested by reducing the cell viability in approximately 70 and 50%, respectively (**Figure 4**). Morphological changes appeared in PC12 cells treated with both SWCNTs and SWCNTs-PEG as shown in **Figure 5**. Cells exposed to SWCNTs showed an elongated shape, which was related to higher toxic effects induced by the untreated CNTs. ROS were generated as a function of both concentration and surface coating after exposure, whereas gene expression analysis showed that the genes involved in oxidoreductases and antioxidant activity, nucleic acid or lipid metabolism and mitochondria dysfunction were highly altered. Interestingly, alteration of the genes was also surface coating-dependent. The authors concluded that surface functionalization of SWCNTs decreases the ROS-mediated toxicological response *in vitro*, corroborating the relevance of surface functionalization in the interaction between nanostructures and biological systems. Likewise, proteins such as type I

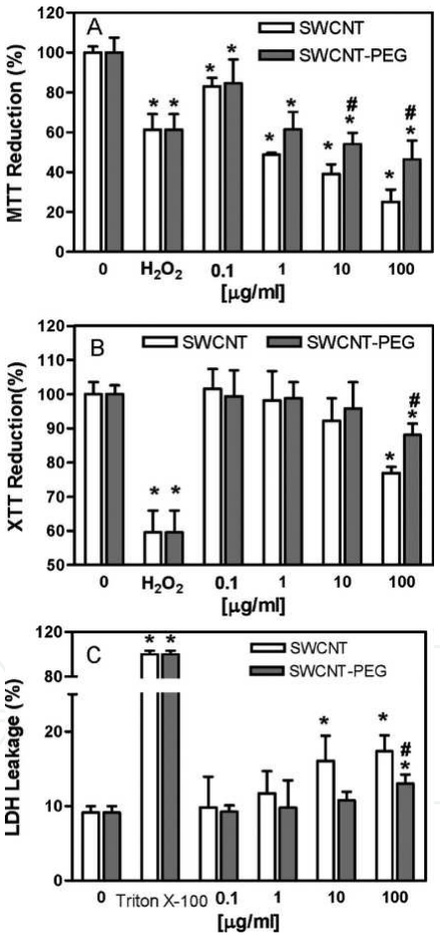

Figure 4. Cytotoxic effect of SWCNTs and SWCNTs-PEG in PC12 cells. Mitochondrial toxicity and membrane damage of neuronal cells incubated with different concentrations of pristine SWCNTs and PEG-coated SWCNTs for 24 h evaluated by MTT (A), XTT (B) and LDH (C) assays. Data are expressed as mean± standard error (n = 3). (*) statistically significant from control; (#) indicates statistically significant within the same concentration group ($p < 0.05$). Adapted with permission from Zhang et al. [61]. Copyright 2011 American Chemical Society.

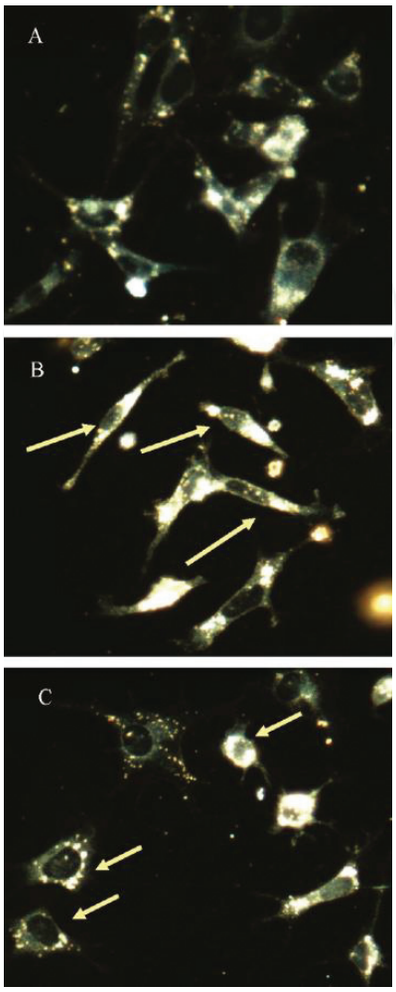

Figure 5. Morphological changes of PC12 cells after 24 h incubation with SWCNTs and SWCNTs-PEG. (A) Normal morphology of the PC12 cells. (B) PC12 cells incubated with SWCNTs present a spindle shape (arrows). (C) SWCNT-PEGs inhibit the dendrite growth (arrows). Adapted with permission from Zhang et al. [61]. Copyright 2011 American Chemical Society.

collagen have shown great potential as surface coting agents in SWCNTs, showing no obvious negative cellular effects and with a high level of internalization taking place through adsorption by the extracellular matrix in bovine articular chondrocytes [62].

Avti et al. showed that SWCNTs synthesized using Gd^{3+} NPs as catalysts induced no structural damage to NIH/3T3 fibroblasts or decreased their viability at concentrations between 1 and 10 μg/mL [53]. In contrast, highly pure SWCNTs triggered similar amounts of pulmonary fibrosis-related compounds interleukin 1β (IL-1β) and transforming growth factor (TGF-β1) in THP-1 and BEAS-2B pulmonary cells without affecting cell viability [63]. Similarly, Di Giorgio et al. studied the cyto- and genotoxic effects, as well as the inflammatory response and ROS production, of SWCNTs on the mouse macrophage cell line RAW 264.7 [64]. There, the authors reported that SWCNTs induced ROS release, cell ultrastructural damage, necrosis and chromosomal aberrations, but did not cause an inflammatory response.

2.3. Multiwalled carbon nanotubes

MWCNTs are defined as a nested coaxial array of SWCNTs, each nanotube being formed by a graphene sheet rolled into a cylinder of nanometer size diameter [65].

It has been postulated that MWCNTs can provide an innovative and promising alternative to conventional drug formulations for cancer therapy, as they can be conjugated with various bioactive molecules such as drugs, surfactants, diagnostic agents and antibodies in order to target receptors that are overexpressed in cancer cells [66–68].

The generation of carboxyl groups by oxidation on the surface of CNTs is one of the most used strategies for introducing hydrophilic moieties onto the CNT hydrophobic surface and in order to conquer a lack of solubility and to improve their biocompatibility [69–71]. Thus, Liu et al. have studied the effects of carboxylated c-MWCNTs on the human normal liver cell line L02 and found a reduction in the toxicity, when compared to pristine MWCNTs with a reduction of around 60% of cell viability at the highest concentration tested after 72 h and concluded that this effect is probably due to a reduced activation of the mitochondria mediated apoptotic pathway [72]. Moreover, as charged entities, c-MWCNTs bind to proteins in the bloodstream through noncovalent interactions to form a protein corona. De Paoli et al. have characterized the interactions of c-MWCNTs with common human proteins such as albumin, fibrinogen, g-immunoglobulins and histone H1 and found that the association of proteins to c-MWCNTs depends on the protein's charge, size and structural flexibility and that it affects the agglomeration state and charge of the CNTs [73].

As with SWCNTs, molecules can be covalently and noncovalently attached to the surface of MWCNTs [74]. The main disadvantage of noncovalent attachment is the lack of biomolecule specificity upon adsorption, which affects the CNTs dispersion stability by replacing the functional surface coating with proteins and molecules contained in all physiological fluids (cell culture media or blood) [65]. Heister et al. have compared five types of CNTs, varying in their dimensions and surface properties, for a multidimensional analysis of dispersion stability and their toxicity toward cancer cells (**Figure 6**), from which it was emphasized that the covalent link between PEG and oxidized MWCNTs leads to stable dispersion and biocompatibility in various biological environments [65].

It has been proposed that the metal impurities trapped inside the MWCNTs may be responsible for their toxicity that partially occurs through the generation of ROS [75]. Fe impurities trapped inside the MWCNTs may be partially responsible for neurotoxicity, as postulated by Meng et al., who investigated and compared the effects of two kinds of MWCNTs with different concentrations of Fe impurities in rat pheochromocytoma PC-12 cells [76]. They found that the exposure to Fe MWCNTs can reduce cell viability up to 80% after 72 h exposure and increase cytoskeletal disruption of undifferentiated PC-12 cells, diminish the ability to form mature neurites and then adversely influence the neuronal dopaminergic phenotype in NGF-treated cells.

Additionally, MWCNTs have been shown to affect the immune system. Pescatori et al. used a whole-genome expression approach to assess whether functionalized MWCNTs could stimulate

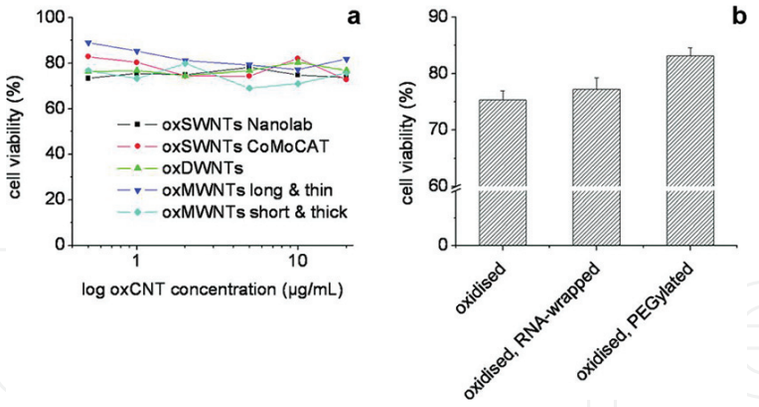

Figure 6. MTT cytotoxicity assay on WiDr human colon cancer cells after being incubated for 96 h with various samples of oxCNTs. No dose-dependent cytotoxicity is observed at this concentration as shown in the range dose-response curves for the five different types of CNTs, displaying (A). Cell viability percentage plot for Nanolab oxidated SWNTs with different surface functionalizations, where PEGylation results in a statistically significant enhancement in cell viability. The cells control correlates with 100% cell viability. Adapted with permission from Heister et al. [74]. Copyright 2010 American Chemical Society.

distinct molecular changes in immune cells, with transcriptomic changes analyzed in human immune cells THP1, a monocytic cell line, Jurkat cells and a T lymphocyte cell line [77]. They found a cell-specific action on monocytes for three types of MWCNTs, which specifically enhanced innate immunity activation mechanisms. The pathways activated are functionally relevant and critical for the development of an effective inflammatory response.

3. Semiconductors

3.1. Titanium dioxide nanoparticles and nanowires

A comprehensive review of the numerous biomedical applications of titanium dioxide (TiO_2) throughout the years was published by Yin et al. [78]. In summary, mostly due to their low cost, strong optical absorption and high chemical stability, TiO_2 NPs have shown great potential in applications such as photodynamic cancer therapy, drug delivery, cell imaging and biosensors, among others.

One of the initial cytotoxicity studies with TiO_2 NPs was performed on human dermal microvascular endothelial cells [79]. There, it was shown that NPs with an average diameter of 70 nm at a dose of 50 μg/mL caused a minor pro-inflammatory response in the form of an increase in the levels of IL-8. Later, a study with mouse fibroblast L929 cells exposed to TiO_2 NPs was conducted by Jin et al. [80]. For 3–600 μg/mL doses, cells appeared to shrink and became round in culture, with a dose-dependent reduction of cell metabolic activity, LDH release and ROS generation. Chromatin fragmentation was also reported, indicating possible DNA damage (**Figure 7**). It was also found that both human neural astrocyte-like U87 cells and human fibroblast HFF-1 cells exposed to 25 nm TiO_2 NPs for 48 h had a decrease in cell survival for doses up to 100 μg/mL, with cell death reported as a combination of apoptosis and necrosis [81]. On the other hand, BEAS-2B cells underwent cell death

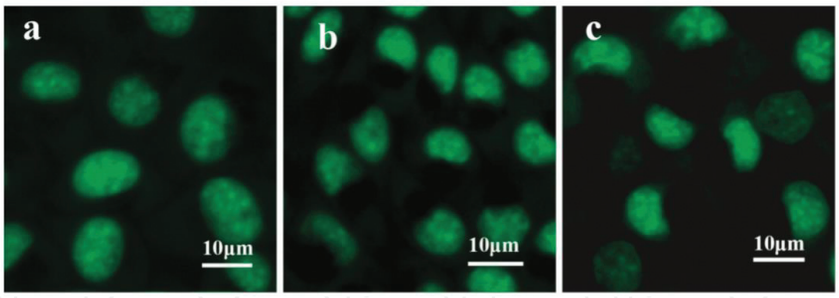

Figure 7. DNA-binding acridine orange staining of L929 mouse fibroblast cells. (A) Control cells with no TiO_2 NPs show normal green nuclei with an organized cellular structure; (B) Cells cultured with 30 μg/mL of TiO_2 NPs show weakly condensed chromatin; and (C) Cells cultured with 600 μg/mL of TiO_2 NPs show fragmented chromatin, an indicator of necrosis. Adapted with permission from Jin et al. [80]. Copyright 2008 American Chemical Society.

through apoptosis, triggered by the activation of caspase-3 and chromatin condensation through ROS [82].

Although the size of single TiO_2 NPs reported by Jin et al. was of 5 nm [80], they were clustered in 20–30 nm aggregates, an effect that could enhance cytotoxicity. It was later shown that there is a correlation between the cytotoxicity of TiO_2 NPs and their aggregate size, as larger aggregates (600 vs. 166 nm) elicited a stronger decrease in cell viability, as well as the expression of genes related to stress and inflammation [83]. In contrast, TiO_2 NPs of 12 nm in diameter aggregated in 450 nm clusters and only at higher doses slightly decreased the viability of glomerular mesangial IP5 and epithelial proximal HK-2 cells, suggesting specific cell responses [84]. Additionally, although ROS was generated in the presence of TiO_2 NPs, the cells were able to maintain their antioxidant potential, thereby showing no oxidative stress.

Cellular uptake studies with 30 nm TiO_2 NPs have been carried out in human amnion epithelial WISH cells using transmission electron microscopy (TEM), with images showing most of the particles localized either inside vesicles or freely in the cytoplasm [85]. In addition to the already mentioned cytotoxic response, WISH cells experience an oxidative response due to ROS accumulation, as well as DNA double strand breaks and cell cycle arrest.

Cytotoxicity data of TiO_2 NWs are scarce, with only a handful of studies published. Magrez et al. observed that TiO_2-based NWs of 5 μm in length and 75 nm in length had a negative impact on the cell proliferation and cell viability of H596 human lung tumor cells in a dose-dependent manner and for concentrations up to 2 μg/mL [86]. NWs were observed to reside in the periphery of the nuclei, which were often enlarged and lobulated or fragmented. In another study, $H_2Ti_3O_7$ NWs at a dose of 10 μg/mL induced the generation of cell debris in eight different cell lines, which the authors associated with an increase in autophagosome-like vacuoles in the cytosol [87].

3.2. Zinc oxide nanoparticles and nanowires

Zinc is a biologically active element that plays a role in different processes, such as the immune system, cell metabolism, cell proliferation, enzymatic function and gene expression, among

others [88, 89]. Due to these biological functions of zinc, coupled with initial biocompatibility studies [90], ease of fabrication and relevant properties [91], zinc oxide (ZnO) nanostructures have been proposed as suitors for several biomedical applications, including cancer cell therapy [92, 93], drug delivery [94, 95] and imaging [96]. However, possible undesirable effects of the interactions between ZnO nanostructures and biological systems could arise and cause a toxicological response. Additionally, ZnO nanostructures are known to dissolve under acidic conditions. The phase-solubility diagram of ZnO [97] indicates that ZnO NPs will dissolve at a pH value below 6.7 at physiological temperature, and they will rapidly dissolve in the acidic pH of the lysosomes (pH 5.7) after their uptake [98]. Zinc oxide NPs can dissolve in an aqueous media to form hydrated Zn^{2+}, which is enhanced in acidic pH as well as in the presence of biological components, such as amino acids and peptides [99]. A review on studies published between the years 2009 and 2011 on the toxicity of ZnO NPs to mammalian cells was reported by Vandebriel et al. [100]. They concluded that the induction of oxidative stress is the most important and the most likely mechanism underlying ZnO NP toxicity.

Initial cytotoxicity studies in human T lymphocytes showed a significant decrease in cell viability only for concentrations higher than 5 mM using ZnO NPs of 13 nm in diameter [101]. It was then found that ZnO NPs preferentially kill cancerous human T lymphocytes compared to normal ones via ROS and apoptosis [92]. Similarly, NPs of the same size were tested against human lung BEAS-2B cells and RAW 264.7 macrophages, and a dose and time-dependent cytotoxicity was found in both cases for doses up to 50 μg/mL and incubation times of 16 h [99]. Moreover, the ZnO NPs were reported to induce the generation of ROS, as well as the activation of the pro-inflammatory marker TNF-α and the pro-inflammatory pathway Jun kinase, as well as intracellular calcium release, a major oxidative stress response. Finally, ZnO NPs were found to reside in caveolae in the case of BEAS-2B cells, whereas in the RAW 264.7 cells, they resided inside lysosomes, with intracellular dissolution and release of Zn^{2+} shown in both cases. In a different study, ZnO NPs also impaired the survival of human neural astrocyte-like U87 cells in a dose-dependent manner [81].

The degree of cytotoxicity of ZnO NPs also depends on their size, as shown by Hanley et al. [102]. Using 4, 13 and 20 nm NPs, they determined an inverse relationship between nanoparticle size and cytotoxicity in terms of cell viability and ROS generation in immune cells. Among these, monocytes were the most sensitive to the ZnO NPs, whereas lymphocytes were the most resistant, as reported previously [101]. In contrast, glomerular mesangial IP5 cells showed a similar dose-dependent decrease in cell viability for ZnO NPs of both <100 nm and >1 μm, along with the generation of ROS [84]. The cell viability of neural stem cells appeared to be indifferent of NP size [103]. In a different work, a differential cytotoxic response was reported, when comparing the effects of 20–30 nm ZnO NPs in human myeloblastic leukemic HL60 cells and normal peripheral blood mononuclear cells (PBMCs) [104]. For concentrations up to 1000 μg/mL, PBMCs maintained a steadily high viable cell population, whereas a dose of 50 μg/mL was enough to bring the cell viability of HL60 cells down to 50%. DNA fragmentation analysis and annexin V staining confirmed that cell death was through the apoptosis pathway. The potent tumor suppressor that regulates the cell cycle and prevents DNA damage, p53 [105], is believed to be a molecular master switch toward apoptosis, and reports show that the p53 pathway was activated in BJ cells (skin fibroblasts) upon ZnO NPs treatment with a concomitant decrease in cell proliferation [106].

The liver, playing a major role in human metabolism, may be a target organ for NPs after they enter into the body. As such, it is an important toxicity evaluation method. Similarly, to previous results, Sharma et al. found that human liver HepG2 cells had a dose-dependent response to ZnO NPs at doses up to 20 μg/mL and for exposure times from 12 to 24 h [107]. Cell death was also shown as being through the apoptotic pathway, due to ROS generation, oxidative stress and mitochondrial and DNA damage. Taken together, all these results suggest that the cytotoxic response to ZnO NPs is dependent on the target cell tissue as well as on changes in NP dimensions.

Kao et al. observed the effects of ZnO NPs of <50 nm in the homeostasis of intracellular Zn^{2+} in human leukemia Jurkat cells and human lung carcinoma H1355 cells and found an increase in the concentration of cytosolic and mitochondrial Zn^{2+}, most probably due to NP dissolution [108], as shown previously [86]. Caspase-3 activation, mitochondrial membrane depolarization and LDH release were also reported, which suggests an apoptotic death pathway due to mitochondrial dysfunction. In a more recent study, the intracellular concentration of Zn^{2+} of breast cancer MDA-MB-231 cells was also increased after treatment with ZnO NPs, leading to the generation of ROS, damage to the cell membrane and mitochondria and culminating in apoptosis [109].

Limited literature exists regarding the biocompatibility of ZnO NWs, but similar cytotoxicity effects as those of NPs were shown by Li et al. using HeLa cells and connective tissue L-929 cells [110]. Although the NWs used were rather large (200 μm in length and 1 μm in diameter), both cell lines seemed to maintain their viability for concentrations up to 10 μg/mL and exposure times of 24 h. Similar viability data were then reported for NWs of 10 μm in length and 327 nm in diameter at the same dose in human macrophages (**Figure 8**) [111]. There, too, it

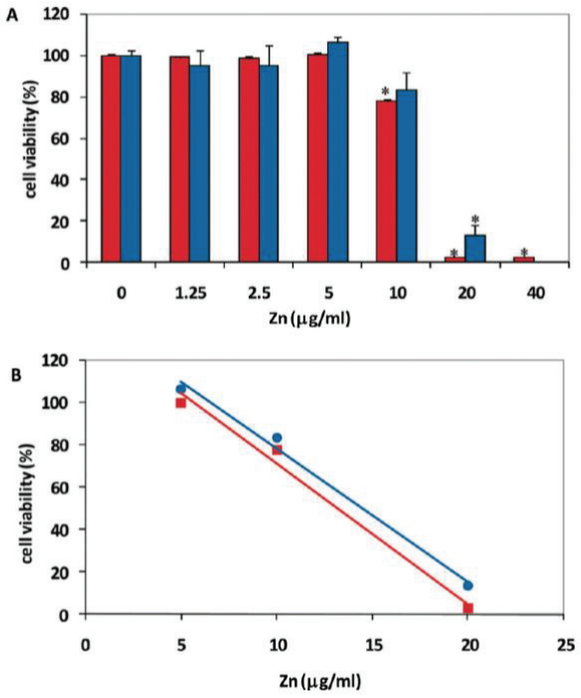

Figure 8. Cytotoxicity of ZnO NWs on HMM human monocyte macrophages. Cell viability was assessed using the neutral red assay, with the red bars denoting doses of Zn in the form of $ZnCl_2$ or ZnO NWs, respectively. Adapted with permission from Müller et al. [111]. Copyright 2010 American Chemical Society.

was found that an intracellular increase of Zn^{2+} precedes cell death, indicating the intracellular dissolution of the ZnO NWs after uptake [112–120].

3.3. Silicon nanoparticles

Coated silicon nanoparticles (Si NPs) have attracted both a great deal of concern and attention, especially in biomedical applications such as disease diagnosis, tumor cell tracking, imaging, drug delivery and gene therapy [121, 122]. They have been widely studied for such applications because of their active surface state and high suspension ability [121, 123, 124]. However, there are some recent reports that limit the use of Si NPs because of potential side effects on the cells, when using them in such a scale and in high concentrations [125].

One of the first studies on Si NPs focused on their cellular uptake [123]. Si NPs were coated with a fluorone dyes called Rhodamine 6G isothiocyanate (RITC), the fluorescence signal of which indicated uptake. NPs of 50 nm diameter at a dose of 80 μg/mL were accumulated in the cytoplasm of HeLa cells after 4 h of incubation at 37°C, while the uptake was reduced by 80% at 4°C. A year later, Lin et al. focused on the toxicity effect of the size, concentration and exposure time of Si NPs on human lung cancer cells (calveolar carcinoma-derived cells) [126]. The cell viability decreased significantly as a function of both nanoparticle dosage (10–100 μg/mL) and exposure time (24, 48 and 72 h). However, the cytotoxicity of two different sizes of Si NPs (15 and 46 nm) did not show a significant difference.

A different study compared the cytotoxicity of a variety of sizes of Si NPs (19, 43, 68 and 498 nm) at 100 μg/mL [127]. After 4 h of incubation with human liver HepG2 cells, it was noticed that the cytotoxicity of Si NPs is size-dependent (i.e., the smaller size the higher cytotoxicity. The live cells were counted by a cell-counting kit (CCK-8). Further, Sahu et al. proved that Si NPs (10–20 nm) are much more toxic than micro-sized ones (0.5–10 μm) for a concentration range of 5–500 μg/mL, after exposing them to human lung epithelial (L-132) and human monocytes (THP-1) for 24 h [128]. The cellular uptake efficiency and pathway of different sized NPs has also been confirmed to be size-dependent, with smaller particles (55 nm) being internalized faster than larger ones (307 nm) [129]. The largest NPs (307 nm) internalized through clathrin-coated pits, whereas medium ones (167 nm) internalized through clathrin-coated vesicles and the smallest (55 nm) were internalized through an energy independent pathway. Despite differences in their internalization pathway, all three sizes showed a high-level of biocompatibility.

In a similar approach as the one of Lin et al., the cytotoxic effects of increasing concentrations of Si NPs (0, 25, 50, 100 and 200 μg/mL) on HepG2 cells were analyzed in terms of ROS level, mitochondrial membrane potential and apoptotic rate. All three tests showed that the level of toxicity of the NPs increases while increasing the concentration from 25 to 100 μg/ml. Additionally, it was shown that the expressions of the apoptotic genes cytC and Caspase-3 were up-regulated with increasing NP concentrations. Additionally, the downregulation of the antiapoptotic Bcl-2 gene and upregulation of the genes p53 and BAX have also been reported [129, 130].

Other approaches have focused on cell-dependent cytotoxicity and surface charge [131]. Kim et al. found that NIH/3T3 fibroblasts appear to be more susceptible to Si NPs in terms of cell

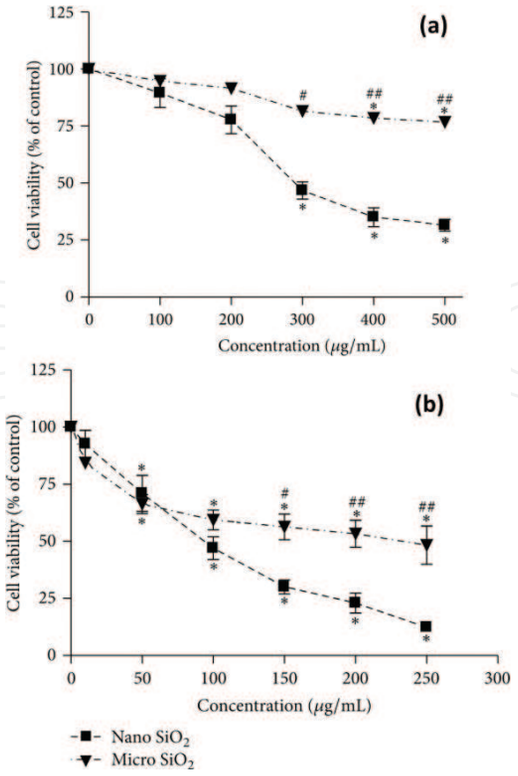

Figure 9. Cytotoxicity of SiO_2 particle is size, concentration and cell-dependent in (a) L-132 cells and (b) THP-1 cells. Results were mean ± SEM of three independent experiments each carried out in triplicate, in comparison to untreated controls. Adapted with permission from Sahu et al. [128]. Copyright 2016 Hindawi Publishing Corporation.

viability, when compared to A549 and HepG2 cells [132]. On the other hand, positively charged (NH_2-coated Si NPs) displayed higher cytotoxicity than negatively charged ones (COOH-coated NPs) in human adenocarcinoma Caco-2 and rat alveolar macrophage NR8383 cells [133]. However, the opposite has also been suggested for HaCaT keratinocyte cells [134]. A summary of the viability dependences on the Si NPs' size, concentration and cell type is shown in **Figure 9** [128].

3.4. Silicon NWs

Si NWs show several advantages over Si NPs. For instance, they tend to not agglomerate in solution compared to Si NPs [135] and they enhance the drug-loading capacity due to their high surface area [136, 137]. However, it has been indicated that Si NWs have more toxic effects to macrophages cells at lower concentrations compared to Si NPs due to the large surface area, which increase the interaction and induce the cell death [138]. Naturally, the concentration of Si NWs plays a role on cell viability. Si NWs of 2 μm long, 55 nm diameter were co-cultured with HeLa and Hep-2 cells at different concentrations [138]. While no toxicity was found on either cell line for concentrations below 190 μg/ml, the cells died and released 75% of their contents into the supernatant at high concentrations (1900 μg/ml) after 72 h of incubation. Zhang et al. used amino-modified (APTES), folate-functionalized Si NWs to study cell interactions [139]. The NWs lengths were between 2.5 and 8.0 μm, with a concentration of

100 μg/mL. It was found that the length of NWs affected the internalization, with NWs longer than 5 μm being more difficult to be internalized, due to geometrical restrictions.

3.5. Quantum dots

Semiconductor quantum dots (QDs) are light-emitting particles that have broad excitation spectra, long fluorescence lifetimes compared to traditional fluorescent probes and are more resistant to photobleaching [140, 141]. Also, they can easily be conjugated to proteins [140], which makes them excellent choices for bioimaging [142–146] and other biomedical applications [141, 147, 148]. Tsoi et al. summarized the toxicity of QDs by two mechanisms: degradation with the release of free cadmium (Cd) and generation of ROS [149]. Each design of QD is a unique combination and has its own physicochemical properties that may influence its biological activity and toxicity. As a result, tremendous research efforts have been devoted to produce high quality QDs by optimizing synthetic procedures, as well as functionalizing their surface in order to enhance biocompatibility [142, 150].

An early study by Derfus et al. demonstrated that CdSe-core QDs oxidized and degraded, releasing Cd ions which induced cell death [151]. When CdSe QDs were exposed to a UV-light for 1, 2, 4 and 8 h and then incubated with hepatocytes, it showed a 6, 42, 83 and 97% decrease in the cells' viability, respectively [143]. Cd is a known carcinogen with potential damage to the renal, skeletal, pulmonary and reproductive systems [152]. Interestingly, Chen et al. showed that the cell viability of HEK293 cells treated with 37.5 nM of 5 nm CdTe QDs was not significantly altered, compared to the control (i.e., untreated cells) after 3 days of incubation [153]. However, high concentrations (300–600 nM) of QDs completely inhibited cell growth from the very beginning. The cytotoxicity of QDs has also been linked to the generation of ROS, which in turn damages cellular proteins, lipids and DNA [149]. The p53 gene was also shown to be inhibited by CdTe QDs, leading to apoptosis and cell death [150].

Tracking the QDs internalization pathways could help explain their toxicological properties. To this end, microscopy studies showed that QDs localize within cellular endosomes and lysosomes, exposing them to an acidic or oxidative microenvironment [149]. It was determined that the hypochlorous acid present in phagocytic cells oxidized polymer-encapsulated CdS and ZnS-capped CdSe QDs, releasing cadmium, zinc, sulfur and selenium into the cytoplasm. Some studies have suggested that the QDs toxicity might derive from multiple factors including the environment and the QDs physicochemical characteristics (such as size, shape and surface chemistry). A surface coating with a ZnS shell [149] or BSA corona [150] reduced the QDs toxicity. In addition, polymeric coatings (i.e., phospholipid-PEG) and inorganic coatings (e.g., Si) can prevent the release of Cd into the biological media [142]. In a different approach, Soenen et al. studied cell viability using Cd-free QDs (ZnSe/ZnS and InP/ZnS QDs) at concentrations ranging from 0 to 100 nM [154]. Cytotoxic effects were observed starting from 60 nM for ZnSe to 80 nM for InP QDs. Further, no increase in cytotoxicity was reported up to 7 days after the initial cell labeling compared to normal QDs due to the absence of Cd.

http://dx.doi.org/10.5772/intechopen.78616

4. Conclusion

Recent studies on the in-vitro cytotoxicity of carbon structure and semiconductors in biomedical applications were reviewed, taking into account nanoparticles and nanowires/nanorods. A summary of the results of representative studies is provided in **Table 1**.

Comparisons between the cytotoxicities of those different nanomaterials are generally difficult to make due to the vast range of methods, concentrations, dimensions, cell lines etc. For instance, the concentrations reported in the different studies were typically evaluated using either ICP or Cryogenic TEM. However, the concentration or dose of the nanomaterial plays a significant role in the cytotoxic response as well as the biomedical applications. Similarly, the reported toxicology of the nanomaterials depends on their interaction with the assay. For example, carbon nanostructures interact with the MTT-formazan crystals but not with XTT or INT reagents.

While the concentrations and exposure times are critical factors, the toxicity of these nanostructures is also material-dependent. These relations can be seen in **Figure 10**, which presents the average values reported for the cell viabilities (ignoring differences in concentrations, incubation times etc.), when exposed to the nanomaterials in the studies covered in **Table 1**. ZnO NPs showed the highest toxicity, while the lowest has been reported for silicon.

In addition, the particle size plays a major role in the cytotoxic properties of the nanostructure, whereby both the cellular uptake efficiency and pathway are affected, with smaller particles being internalized faster than the larger ones.

The induction of ROS after dissolving the nanostructures in the lysosomes was shown to be the primary underlying cause of the toxicity in several cases, leading to cell death through the apoptotic pathway, due to ROS generation and mitochondrial damage. The acidic condition inside the lysosome increases the digestion of the particles, enhancing the release of ions that affect the viability of the cells. This is a particularly relevant issue in case of CdSe-core QDs, which release Cd ions upon oxidation, leading to fast cell death.

Adding a coating to the nanostructure typically affected both the toxicity and the surface charge of the nanostructure, where cationic surfaces are more toxic than anionic. For instance, the toxicity of QDs was reduced by adding a BSA corona, and the release of Cd was prevented by the addition of polymeric and inorganic coatings. The type of the coatings was shown to affect the cell viability differently.

The cytotoxicity of the nanomaterial depends also on the nanostructure's shape. In this regard, several advantages have been reported for NWs over NPs. For instance, they enhance the drug-loading capacity due to their large surface area. An interesting observation from **Figure 10** is that NWs/NRs are, on average, less cytotoxic than NPs, with titanium dioxide being the only exception. However, one study has shown that the large surface area of Si NWs has a more toxic effect at lower concentrations compared to NPs. This was attributed to the increased interaction of the nanomaterial with the cells due to the large surface area.

Nanostructure type	Surface coating	Nanostructure concentration	Average size	Cell line	Cell viability	Viability test	Reference
C_{60}	Pristine, $C_{60}(OH)_{12}$, $C_{60}(OH)_{24}$,	0.125 mM/1 h	N/A	rat hepatocytes	80% for pristine, $C_{60}(OH)_{12}$ and 60% for $C_{60}(OH)_{24}$.	Tryptan blue/ microscopy, MPP, GSH	[35]
C_{60}	C_{60}-alanine, -NO_2, -PVP, -NO_2-proline, sodium salt of a polycarboxylic derivative	0.001–0.2 mg/mL for C_{60}-NO_2-proline and 0.016–0.2 mg/mL for all others/48 h	N/A	HEp-2 cells	No cytotoxicity except for the sodium salt of a polycarboxylic derivative with 20% viability at 0.01 mg/mL	Crystal violet/optical density	[44]
C_{60}	PEG of various sizes	0.03–1 mg/mL/24 h	N/A	HepG2, NHDF, Caco2, HUVEC, U931, J774 A1	Maximum inhibition at 1 mg/ ml of Full–PEG2000 for J774 (41%) and U937 (62%).	MTT, LDH assays	[45]
SWCNTs	Pristine and PEG	0.1–100 μg/mL/ 24 h	0.7–1.6 nm diameter, 0.2–3 μm length	PC12 cells	30 and 50% viability in MTT at highest concentration, respectively. Higher values for XTT and 10–20% LDH leakage	MTT, XTT, LDH, DCF, GSH assays	[58]
SWCNTs	Collagen	15 μg/mL/4 h to 15 days.	0.7–1.6 nm diameter, N/ A	BACs	No cytotoxicity	WST-1 assay, Live/dead	[59]
SWCNTs	Gd-NPs as catalysts and PEG	50–100 μg/mL/12–48 h	N/A	NIH/3 T3 fibroblasts	70% viability at highest concentration and time exposure	Tryptan blue/ microscopy, Live/dead	[55]
MWCNTs	Pristine, COOH	12.5–200 μg/mL/ 24, 48 and 72 h	10–20 nm diameter, 10–30 μm length	human normal liver cell line L02	60 and 80% viability at highest concentration and time exposure, respectively	CellTiter-GloV® assay	[68]
MWCNTs	3 and 23% of Fe impurities	5–60 μg/mL/24, 48 and 72 h	2–50 nm diameter, 50 μm length	PC12 cells	70 and 20% viability at highest concentration and time exposure, respectively	CCK-8	[73]
TiO_2 NPs	—	600 μg/mL	5 nm diameter	L929 mouse fibroblast cells	<70%	MTT assay	[107]

Nanostructure type	Surface coating	Nanostructure concentration	Average size	Cell line	Cell viability	Viability test	Reference
ZnO NPs	—	10 mM	13 nm diameter	Human T lymphocytes	40%	Propidium iodide staining	[110]
SiO_2 NPs	—	50 μg/mL	10–20 nm	monocytes (THP-1) cells	71%	MTT assay	[124]
Si NPs	Coated with negatively charged (COOH)	3 mg/ml	1.6 nm	Rat alveolar macrophage NR8383 cells	No cytotoxicity	MTT assay	[132]
Si NPs	Coated with positively charged ($NH_{2)}$	0–100 mg/ml	3.9 nm	Rat alveolar macrophage NR8383 cells	The EC50 values = 0.38 μg/ml	MTT assay	[129]
Si NPs	—	160 μg/ml	7 nm	HepG2 cells	~98%	MTT assay	[136]
Si NPs	—	160 μg/ml	20 nm	HepG2 cells	~72%	MTT assay	[153]
Si NPs	—	160 μg/ml	50 nm	HepG2 cells	~49%	MTT assay	[156]
Si NWs	—	<190 μg/ml	2 μm long, 55 nm diameter	HeLa and Hep-2 cells	75%	MTT assay	[152]
Si NWs	—	1 μg/ml	500 nm long, 100 nm diameter	breast cancer cells line (MCF-7/ADR)	90%	MTT assay	[154]
Si NW arrays	—	—	5 μm long, 20–100 nm diameter	HeLa cells	98%	MTT assay	[155]
Si NW arrays	Coated with AgNPs	—	5 μm long, 20–100 nm diameter	HeLa cells	80%	MTT assay	[156]
Si NW arrays	Coated with Cu NPs	—	5 μm long, 20–100 nm diameter	HeLa cells	~50%	MTT assay	[156]

Nanostructure type	Surface coating	Nanostructure concentration	Average size	Cell line	Cell viability	Viability test	Reference
CdSe QDs	Oxidation for 0 h, 1 h, 2 h and 4 h	62.5 μg/mL	7 nm	Hepatocyte cells	100, 98.55 and 21%, respectively	MTT assay	[152]
CdTe QDs	—	37.5 and 75 nM	5 nm	HEK293 cells	∼87 and ∼67%	MTT assay	[154]
ZnSe QDs	Cd-free	60 nM	1–10 nm	HUVEC cells	∼77%	Alamar Blue assay	[155]
InP QDs	Cd-free	80 nM	1–10 nm	HUVEC cells	∼78%	Alamar Blue assay	[155]

Table 1. Summary of in-vitro cytotoxicity studies with different kinds of nanoparticles (NPs) and nanowires (NWs), NWs with aspect ratio <10 are often called nanorods (NR), SWCNT the abbreviation of single-walled carbon nanotube, MWCNT for multiwalled carbon nanotube and QD for quantum dots.

http://dx.doi.org/10.5772/intechopen.78616

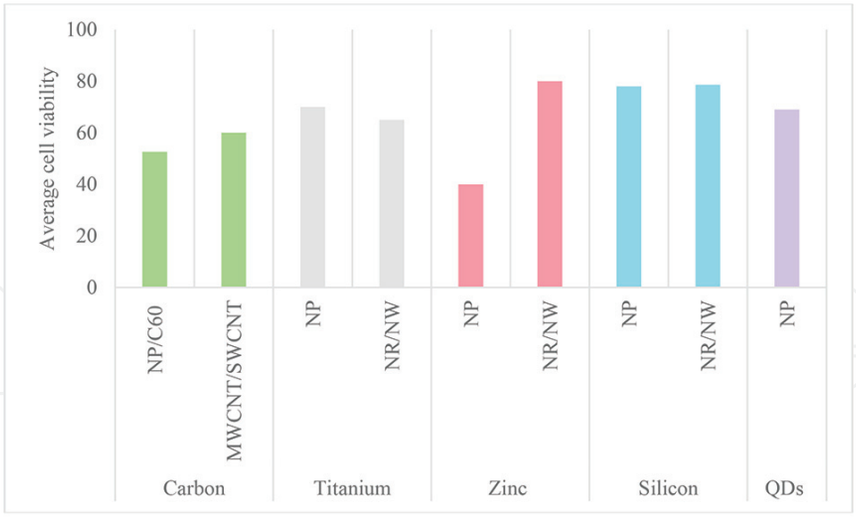

Figure 10. Average cell viability when exposed to nanomaterials reported in **Table 1**, considering nanoparticles (NP), nanorods (NR), nanowires (NW), Fullerene (C_{60}), single-walled carbon nanotubes (SWCNT), multiwalled carbon nanotubes (MWCNT) and Quantum Dots (QDs).

While all these studies contributed to obtain a better picture of the cytotoxicity of nanomaterials and the underlying mechanisms, it is a persisting issue that a consistent measurement and reporting system will be needed for future studies. This will not only enable performing more accurate comparisons of the toxicological characteristics of nanostructures, but also to better evaluate the potential of using them for biomedical applications.

Acknowledgements

Research reported in this publication was supported by the King Abdullah University of Science and Technology (KAUST).

Policy: https://www.intechopen.com/authorship-policy.html.

Author details

Jose E. Perez[1,2], Nouf Alsharif[1,2], Aldo I. Martínez-Banderas[1,2], Basmah Othman[1], Jasmeen Merzaban[1], Timothy Ravasi[1] and Jürgen Kosel[2]*

*Address all correspondence to: jurgen.kosel@kaust.edu.sa

1 Division of Biological and Environmental Sciences and Engineering, King Abdullah University of Science and Technology, Thuwal, Kingdom of Saudi Arabia

2 Division of Computer, Electrical and Mathematical Sciences and Engineering, King Abdullah University of Science and Technology, Thuwal, Kingdom of Saudi Arabia

References

[1] ASTM International. Standard Terminology Relating to Nanotechnology [Internet]. 2012. Available from: https://www.astm.org/Standards/E2456.htm [Accessed: March 15, 2018]

[2] Sanvicens N, Marco MP. Multifunctional nanoparticles—Properties and prospects for their use in human medicine. Trends in Biotechnology. 2008;**26**:425-433. DOI: 10.1016/j.tibtech.2008.04.005

[3] Sau TK, Rogach AL, Jäckel F, Klar TA, Feldmann J. Properties and applications of colloidal nonspherical noble metal nanoparticles. Advanced Materials. 2010;**22**:1805-1825. DOI: 10.1002/adma.200902557

[4] Brigger I, Dubernet C, Couvreur P. Nanoparticles in cancer therapy and diagnosis. Advanced Drug Delivery Reviews. 2002;**54**:631-651. DOI: 10.1016/S0169-409X(02)00044-3

[5] Doane TL, Burda C. The unique role of nanoparticles in nanomedicine: Imaging, drug delivery and therapy. Chemical Society Reviews. 2012;**41**:2885. DOI: 10.1039/c2cs15260f

[6] Parveen S, Misra R, Sahoo SK. Anoparticles: A boon to drug delivery, therapeutics, diagnostics and imaging. Nanomedicine: Nanotechnology, Biology and Medicine. 2012; **8**:147-166. DOI: 10.1016/j.nano.2011.05.016

[7] Li L, Jiang W, Luo K, Song H, Lan F, Wu Y, Gu Z. Superparamagnetic iron oxide nanoparticles as MRI contrast agents for non-invasive stem cell labeling and tracking. Theranostics. 2013;**3**:595-615. DOI: 10.7150/thno.5366

[8] Xie H, Zhu Y, Jiang W, Zhou Q, Yang H, Gu N, Zhang Y, Xu H, Xu H, Yang X. Lactoferrin-conjugated superparamagnetic iron oxide nanoparticles as a specific MRI contrast agent for detection of brain glioma *in vivo*. Biomaterials. 2011;**32**:495-502. DOI: 10.1016/j.biomaterials.2010.09.024

[9] Kuo S-W, Lin H-I, Ho JH-C, Shih Y-R V, Chen H-F, Yen T-J, Lee OK. Regulation of the fate of human mesenchymal stem cells by mechanical and stereo-topographical cues provided by silicon nanowires. Biomaterials. 2012;**33**:5013-5022. DOI: 10.1016/j.biomaterials.2012.03.080

[10] Liu D, Yi C, Wang K, Fong CC, Wang Z, Lo PK, Sun D, Yang M. Reorganization of cytoskeleton and transient activation of Ca^{+2} channels in mesenchymal stem cells cultured on silicon nanowire arrays. ACS Applied Materials & Interfaces. 2013;**5**:13295-13304. DOI: 10.1021/am404276r

[11] Liu D, Yi C, Fong C-C, Jin Q, Wang Z, Yu W-K, Sun D, Zhao J, Yang M. Activation of multiple signaling pathways during the differentiation of mesenchymal stem cells cultured in a silicon nanowire microenvironment. Nanomedicine: Nanotechnology, Biology and Medicine. 2014:1-11. DOI: 10.1016/j.nano.2014.02.003

[12] Laurent S, Dutz S, Häfeli UO, Mahmoudi M. Magnetic fluid hyperthermia: Focus on superparamagnetic iron oxide nanoparticles. Advances in Colloid and Interface Science. 2011;**166**:8-23. DOI: 10.1016/j.cis.2011.04.003

[13] Cherukuri P, Glazer ES, Curley SA. Targeted hyperthermia using metal nanoparticles. Advanced Drug Delivery Reviews. 2010;**62**:339-345. DOI: 10.1016/j.addr.2009.11.006

[14] Su Y, Wei X, Peng F, Zhong Y, Lu Y, Su S, Xu T, Lee ST, He Y. Gold nanoparticles-decorated silicon nanowires as highly efficient near-infrared hyperthermia agents for cancer cells destruction. Nano Letters. 2012;**12**:1845-1850. DOI: 10.1021/nl204203t

[15] Fung AO, Kapadia V, Pierstorff E, Ho D, Chen Y. Induction of cell death by magnetic actuation of nickel nanowires internalized by fibroblasts. Journal of Physical Chemistry C. 2008;**112**:15085-15088. DOI: 10.1021/jp806187r

[16] Contreras MF, Sougrat R, Zaher A, Ravasi T, Kosel J. Non-chemotoxic induction of cancer cell death using magnetic nanowires. International Journal of Nanomedicine. 2015;**10**: 2141-2153. DOI: 10.2147/IJN.S77081

[17] Dreaden EC, Mwakwari SC, Austin LA, Kieffer MJ, Oyelere AK, El-Sayed MA. Small molecule-gold nanorod conjugates selectively target and induce macrophage cytotoxicity towards breast cancer cells. Small. 2012;**8**:2819-2822. DOI: 10.1002/smll.201200333

[18] Cortajarena AL, Ortega D, Ocampo SM, Gonzalez-García A, Couleaud P, Miranda R, Belda-Iniesta C, Ayuso-Sacido A. Engineering iron oxide nanoparticles for clinical settings. Nano. 2014;**1**. DOI: 10.5772/58841

[19] Liu Y, Zhao Y, Sun B, Chen C. Understanding the toxicity of carbon nanotubes. Accounts of Chemical Research. 2013;**46**:702-713. DOI: 10.1021/ar300028m

[20] Kong B, Seog JH, Graham LM, Lee SB. Experimental considerations on the cytotoxicity of nanoparticles. Nanomedicine. 2011;**6**:929-941. DOI: 10.2217/nnm.11.77

[21] Gratton SE, Ropp P, Pohlhaus PD, Luft JC, Madden VJ, Napier ME, JM DS. The effect of particle design on cellular internalization pathways. Proceedings of the National Academy of Sciences of the United States of America. 2008;**105**:11613-11618. DOI: 10.1073/pnas.0801763105

[22] Fröhlich E. The role of surface charge in cellular uptake and cytotoxicity of medical nanoparticles. International Journal of Nanomedicine. 2012;**7**:5577-5591. DOI: 10.2147/IJN.S36111

[23] Kim ST, Saha K, Kim C, Rotello VM. The role of surface functionality in determining nanoparticle cytotoxicity. Accounts of Chemical Research. 2013;**46**:681-691. DOI: 10.1021/ar3000647

[24] Lewinski N, Colvin V, Drezek R. Cytotoxicity of nanoparticles. Small (Weinheim an der Bergstrasse, Germany). 2008;**4**:26-49. DOI: 10.1002/smll.200700595

[25] Zhao F, Zhao Y, Liu Y, Chang X, Chen C, Zhao Y. Cellular uptake, intracellular trafficking, and cytotoxicity of nanomaterials. Small. 2011;**7**:1322-1337. DOI: 10.1002/smll.201100001

[26] Martin N, Guldi DM, Echegoyen L. Carbon nanostructures—Introducing the latest web themed issue. Chemical Communications. 2011;**47**:604-605. DOI: 10.1039/c0cc90122a

[27] Kroto HW, Heath JR, O'Brien SC, Curl RF, Smalley RE. C60: Buckminsterfullerene. Nature. 1985;**318**:162-163. DOI: 10.1038/318162a0

[28] Iijima S. Helical microtubules of graphitic carbon. Nature. 1991;**354**:56-58. DOI: 10.1038/354056a0

[29] Kurkina T, Balasubramanian K. Towards in vitro molecular diagnostics using nanostructures. Cellular and Molecular Life Sciences. 2012;**69**:373-388. DOI: 10.1007/s00018-011-0855-7

[30] Prakash S, Malhotra M, Shao W, Tomaro-Duchesneau C, Abbasi S. Polymeric nanohybrids and functionalized carbon nanotubes as drug delivery carriers for cancer therapy. Advanced Drug Delivery Reviews. 2011;**63**:1340-1351. DOI: 10.1016/j.addr.2011.06.013

[31] Liang F, Chen B. A review on biomedical applications of single-walled carbon nanotubes. Current Medicinal Chemistry. 2010;**17**:10-24. DOI: 10.2174/092986710789957742

[32] Zhu L, Schrand AM, Voevodin AA, Chang DW, Dai LM, Hussain SM. Assessment of human lung macrophages after exposure to multi-walled carbon nanotubes. Part II. DNA damage. Nanoscience and Nanotechnology Letters. 2011;**3**:94-98. DOI: 10.1166/nnl.2011.1126

[33] Iancu C, Mocan L. Advances in cancer therapy through the use of carbon nanotube-mediated targeted hyperthermia. International Journal of Nanomedicine. 2011;**6**:2543. DOI: 10.2147/ijn.s27335

[34] Tarakanov AO, Goncharova LB, Tarakanov YA. Carbon nanotubes towards medicinal biochips. Wiley Interdisciplinary Reviews. Nanomedicine and Nanobiotechnology. 2010; **2**:1-10. DOI: 10.1002/wnan.69

[35] Hartman KB, Wilson LJ. Carbon nanostructures as a new high-performance platform for MR molecular imaging. In: Chan WCW, editor. Handbook of Bio Applications of Nanoparticles. Berlin: Springer-Verlag; 2007. pp. 74-84. DOI: 10.1007/978-0-387-76713-0

[36] Lacerda L, Russier J, Pastorin G, Herrero MA, Venturelli E, Dumortier H, Al-Jamal KT, Prato M, Kostarelos K, Bianco A. Translocation mechanisms of chemically functionalised carbon nanotubes across plasma membranes. Biomaterials. 2012;**33**:3334-3343. DOI: 10.1016/j.biomaterials.2012.01.024

[37] Wong BS, Yoong SL, Jagusiak A, Panczyk T, Ho HK, Ang WH, Pastorin G. Carbon nanotubes for delivery of small molecule drugs. Advanced Drug Delivery Reviews. 2013;**65**:1964-2015. DOI: 10.1016/j.addr.2013.08.005

[38] Nakagawa Y, Suzuki T, Ishii H, Nakae D, Ogata A. Cytotoxic effects of hydroxylated fullerenes on isolated rat hepatocytes via mitochondrial dysfunction. Archives of Toxicology. 2011;**85**:1429-1440. DOI: 10.1007/s00204-011-0688-z

[39] Kato H, Kanazawa Y, Okumura M, Taninaka A, Yokawa T, Shinohara H. Lanthanoid Endohedral Metallofullerenols for MRI contrast agents. Journal of the American Chemical Society. 2003;**125**:4391-4397. DOI: 10.1021/ja027555+

[40] Fan J, Fang G, Zeng F, Wang X, Wu S. Water-dispersible fullerene aggregates as a targeted anticancer prodrug with both chemo- and photodynamic therapeutic actions. Small. 2013;**9**:613-621. DOI: 10.1002/smll.201201456

[41] Raoof M, Mackeyev Y, Cheney MA, Wilson LJ, Curley SA. Internalization of C60 fullerenes into cancer cells with accumulation in the nucleus via the nuclear pore complex. Biomaterials. 2012;**33**:2952-2960. DOI: 10.1016/j.biomaterials.2011.12.043

[42] Krishna V, Stevens N, Koopman B, Moudgil B. Optical heating and rapid transformation of functionalized fullerenes. Nature Nanotechnology. 2010;**5**:330-334. DOI: 10.1038/nnano.2010.35

[43] Borm PJA, Robbins D, Haubold S, Kuhlbusch T, Fissan H, Donaldson K, Schins R, Stone V, Kreyling W, Lademann J, Krutmann J, Warheit D, Oberdorster E. The potential risks of nanomaterials: A review carried out for ECETOC. Particle and Fibre Toxicology. 2006;**3**:1-35. DOI: 10.1186/1743-8977-3-11

[44] Lucafò M, Gerdol M, Pallavicini A, Pacor S, Zorzet S, Da Ros T, Prato M, Sava G. Profiling the molecular mechanism of fullerene cytotoxicity on tumor cells by RNA-seq. Toxicology. 2013;**314**:183-192. DOI: 10.1016/j.tox.2013.10.001

[45] Nakagawa Y, Suzuki T, Nakajima K, Inomata A, Ogata A, Nakae D. Effects of N-acetyl-l-cysteine on target sites of hydroxylated fullerene-induced cytotoxicity in isolated rat hepatocytes. Archives of Toxicology. 2014;**88**:115-126. DOI: 10.1007/s00204-013-1096-3

[46] Shimizu K, Kubota R, Kobayashi N, Tahara M, Sugimoto N, Nishimura T, Ikarashi Y. Cytotoxic effects of hydroxylated fullerenes in three types of liver cells. Materials. 2013;**6**:2713-2722. DOI: 10.3390/ma6072713

[47] Bobylev AG, Okuneva AD, Bobyleva LG, Fadeeva IS, Fadeev RS, Salmov NN, Podlubnaya ZA. Study of citotoxicity of fullerene C-60 derivatives. Biofizika. 2012;**57**:746-750. DOI: 10.1134/S0006350912050041

[48] Canape C, Foillard S, Bonafe R, Maiocchi A, Doris E. Comparative assessment of the in vitro toxicity of some functionalized carbon nanotubes and fullerenes. RSC Advances. 2015;**5**:68446-68453. DOI: 10.1039/C5RA11489F

[49] Monticelli L, Salonen E, Ke PC, Vattulainen I. Effects of carbon nanoparticles on lipid membranes: A molecular simulation perspective. Soft Matter. 2009;**5**:4433-4445. DOI: 10.1039/B912310E

[50] Mohandas N, Gallagher PG. Red cell membrane: Past, present, and future. Blood. 2008;**112**:3939-3948. DOI: 10.1182/blood-2008-07-161166

[51] Grebowski J, Krokosz A, Puchala M. Membrane fluidity and activity of membrane ATPases in human erythrocytes under the influence of polyhydroxylated fullerene. Biochimica et Biophysica Acta-Biomembranes. 2013;**1828**:241-248. DOI: 10.1016/j.bbamem.2012.09.008

[52] Pantarotto D, Singh R, McCarthy D, Erhardt M, Briand J-P, Prato M, Kostarelos K, Bianco A. Functionalized carbon nanotubes for plasmid DNA gene delivery. Angewandte Chemie, International Edition. 2004;**43**:5242-5246. DOI: 10.1002/anie.200460437

[53] Dai H. Carbon nanotubes: Synthesis, integration, and properties. Accounts of Chemical Research. 2002;**35**:1035-1044. DOI: 10.1021/ar0101640

[54] Prakash S, Kulamarva AG. Recent advances in drug delivery: Potential and limitations of carbon nanotubes. Recent Patents on Drug Delivery & Formulation. 2007;**1**:214-221. DOI: 10.2174/187221107782331601

[55] Prato M, Kostarelos K, Bianco A. Functionalized carbon nanotubes in drug design and discovery. Accounts of Chemical Research. 2008;**41**:60-68. DOI: 10.1021/ar700089b

[56] Mo Y, Wang H, Liu J, Lan Y, Guo R, Zhang Y, Xue W, Zhang Y. Controlled release and targeted delivery to cancer cells of doxorubicin from polysaccharide-functionalised single-walled carbon nanotubes. Journal of Materials Chemistry B. 2015;**3**:1846-1855. DOI: 10.1039/C4TB02123A

[57] Madani SY, Naderi N, Dissanayake O, Tan A, Seifalian AM. A new era of cancer treatment: Carbon nanotubes as drug delivery tools. International Journal of Nanomedicine. 2011;**6**:2963-2979. DOI: 10.2147/ijn.s16923

[58] Avti PK, Caparelli ED, Sitharaman B. Cytotoxicity, cytocompatibility, cell-labeling efficiency, and in vitro cellular magnetic resonance imaging of gadolinium-catalyzed single-walled carbon nanotubes. Journal of Biomedical Materials Research. Part A. 2013;**101**: 3580-3591. DOI: 10.1002/jbm.a.34643

[59] Arnold MS, Green AA, Hulvat JF, Stupp SI, Hersam MC. Sorting carbon nanotubes by electronic structure using density differentiation. Nature Nanotechnology. 2006;**1**:60-65. DOI: 10.1038/nnano.2006.52

[60] Charlier J-C, Blase X, Roche S. Electronic and transport properties of nanotubes. Reviews of Modern Physics. 2007;**79**:677-732. DOI: 10.1103/RevModPhys.79.677

[61] Zhang Y, Xu Y, Li Z, Chen T, Lantz SM, Howard PC, Paule MG, Slikker W, Watanabe F, Mustafa T, Biris AS, Ali SF. Mechanistic toxicity evaluation of uncoated and PEGylated single-walled carbon nanotubes in neuronal PC12 cells. ACS Nano. 2011;**5**:7020-7033. DOI: 10.1021/nn2016259

[62] Mao H, Kawazoe N, Chen G. Uptake and intracellular distribution of collagen-functionalized single-walled carbon nanotubes. Biomaterials. 2013;**34**:2472-2479. DOI: 10.1016/j.biomaterials.2013.01.002

[63] Wang X, Mansukhani ND, Guiney LM, Lee J-H, Li R, Sun B, Liao Y-P, Chang CH, Ji Z, Xia T, Hersam MC, Nel AE. Toxicological profiling of highly purified metallic and semiconducting single-walled carbon nanotubes in the rodent lung and *E. coli*. ACS Nano. 2016;**10**:6008-6019. DOI: 10.1021/acsnano.6b01560

[64] Di Giorgio ML, Bucchianico, Di S, Ragnelli AM, Aimola P, Santucci S, Poma A. Effects of single and multi walled carbon nanotubes on macrophages: Cyto and genotoxicity and electron microscopy. Mutation Research, Genetic Toxicology and Environmental Mutagenesis. 2011;**722**:20-31. DOI: 10.1016/j.mrgentox.2011.02.008

[65] Dresselhaus MS, Endo M. Relation of carbon nanotubes to other carbon materials. In: Dresselhaus A, Dresselhaus G, Avouris P, editors. Handbook of Carbon Nanotubes Synthesis, Structure, Properties, and Applications. Berlin, Heidelberg: Springer; 2001. pp. 11-28. DOI: 10.1007/3–540-39947-x_2

[66] Datir SR, Das M, Singh RP, Jain S. Hyaluronate tethered, "smart" multiwalled carbon nanotubes for tumor-targeted delivery of doxorubicin. Bioconjugate Chemistry. 2012;**23**: 2201-2213. DOI: 10.1021/bc300248t

[67] Das M, Datir SR, Singh RP, Jain S. Augmented anticancer activity of a targeted, intracellularly activatable, theranostic nanomedicine based on fluorescent and radiolabeled, methotrexate-folic acid-multiwalled carbon nanotube conjugate. Molecular Pharmaceutics. 2013; **10**:2543-2557. DOI: 10.1021/mp300701e

[68] Arya N, Arora A, Vasu KS, Sood AK, Katti DS. Combination of single walled carbon nanotubes/graphene oxide with paclitaxel: A reactive oxygen species mediated synergism for treatment of lung cancer. Nanoscale. 2013;**5**:2818-2829. DOI: 10.1039/C3NR33190C

[69] Bianco A, Kostarelos K, Prato M. Applications of carbon nanotubes in drug delivery. Current Opinion in Chemical Biology. 2005;**9**:674-679. DOI: 10.1016/j.cbpa.2005.10.005

[70] Wu W, Wieckowski S, Pastorin G, Benincasa M, Klumpp C, Briand J-P, Gennaro R, Prato M, Bianco A. Targeted delivery of Amphotericin B to cells by using functionalized carbon nanotubes. Angewandte Chemie, International Edition. 2005;**44**:6358-6362. DOI: 10.1002/anie.200501613

[71] Liu Z, Dong X, Song L, Zhang H, Liu L, Zhu D, Song C, Leng X. Carboxylation of multiwalled carbon nanotube enhanced its biocompatibility with L02 cells through decreased activation of mitochondrial apoptotic pathway. Journal of Biomedical Materials Research Part A. 2014;**102**:665-673. DOI: 10.1002/jbm.a.34729

[72] De Paoli SH, Diduch LL, Tegegn TZ, Orecna M, Strader MB, Karnaukhova E, Bonevich JE, Holada K, Simak J. The effect of protein corona composition on the interaction of carbon nanotubes with human blood platelets. Biomaterials. 2014;**35**:6182-6194. DOI: 10.1016/j.biomaterials.2014.04.067

[73] Wenrong Y, Pall T, Gooding JJ, Simon PR, Filip B. Carbon nanotubes for biological and biomedical applications. Nanotechnology. 2007;**18**:412001. DOI: 10.1088/0957-4484/18/41/412001

[74] Heister E, Lamprecht C, Neves V, Tîlmaciu C, Datas L, Flahaut E, Soula B, Hinterdorfer P, Coley HM, Silva SRP, McFadden J. Higher dispersion efficacy of functionalized carbon nanotubes in chemical and biological environments. ACS Nano. 2010;**4**:2615-2626. DOI: 10.1021/nn100069k

[75] Smart SK, Cassady AI, Lu GQ, Martin DJ. The biocompatibility of carbon nanotubes. Carbon. 2006;**44**:1034-1047. DOI: 10.1016/j.carbon.2005.10.011

[76] Meng L, Jiang A, Chen R, Li C, Wang L, Qu Y, Wang P, Zhao Y, Chen C. Inhibitory effects of multiwall carbon nanotubes with high iron impurity on viability and neuronal differentiation in cultured PC12 cells. Toxicology. 2013;**313**:49-58. DOI: 10.1016/j.tox.2012.11.011

[77] Pescatori M, Bedognetti D, Venturelli E, Ménard-Moyon C, Bernardini C, Muresu E, Piana A, Maida G, Manetti R, Sgarrella F, Bianco A, Delogu LG. Functionalized carbon nanotubes as immunomodulator systems. Biomaterials. 2013;**34**:4395-4403. DOI: 10.1016/j.biomaterials.2013.02.052

[78] Yin ZF, Wu L, Yang HG, Su YH. Recent progress in biomedical applications of titanium dioxide. Physical Chemistry Chemical Physics (PCCP). 2013;**15**:4844-4858. DOI: 10.1039/c3cp43938k

[79] Peters K, Unger RE, Kirkpatrick CJ, Gatti AM, Monari E. Effects of nano-scaled particles on endothelial cell function in vitro: Studies on viability, proliferation and inflammation. Journal of Materials Science: Materials in Medicine. 2004;**15**:321-325

[80] Jin CY, Zhu BS, Wang XF, Lu QH. Cytotoxicity of titanium dioxide nanoparticles in mouse fibroblast cells. Chemical Research in Toxicology. 2008;**21**:1871-1877. DOI: 10.1021/tx800179f

[81] Lai JCK, Lai MB, Jandhyam S, Dukhande VV, Bhushan A, Daniels CK, Leung SW. Exposure to titanium dioxide and other metallic oxide nanoparticles induces cytotoxicity on human neural cells and fibroblasts. International Journal of Nanomedicine. 2008;**3**: 533-545. DOI: 10.2147/IJN.S3234

[82] Park E-J, Yi J, Chung K-H, Ryu D-Y, Choi J, Park K. Oxidative stress and apoptosis induced by titanium dioxide nanoparticles in cultured BEAS-2B cells. Toxicology Letters. 2008;**180**:222-229. DOI: 10.1016/j.toxlet.2008.06.869

[83] Okuda-Shimazaki J, Takaku S, Kanehira K, Sonezaki S, Taniguchi A. Effects of titanium dioxide nanoparticle aggregate size on gene expression. International Journal of Molecular Sciences. Jun. 2010;**11**:2383-2392. DOI: 10.3390/ijms11062383

[84] Pujalté I, Passagne I, Brouillaud B, Tréguer M, Durand E, Ohayon-Courtès C, L'Azou B. Cytotoxicity and oxidative stress induced by different metallic nanoparticles on human kidney cells. Particle and Fibre Toxicology. 2011;**8**:10. DOI: 10.1186/1743-8977-8-10

[85] Saquib Q, Al-Khedhairy AA, Siddiqui MA, Abou-Tarboush FM, Azam A, Musarrat J. Titanium dioxide nanoparticles induced cytotoxicity, oxidative stress and DNA damage in human amnion epithelial (WISH) cells. Toxicology in Vitro. 2012;**26**:351-361. DOI: 10.1016/j.tiv.2011.12.011

[86] Magrez A, Horváth L, Smajda R, Salicio V, Pasquier N, Forró L, Schwaller B. Cellular toxicity of TiO_2-based nanofilaments. ACS Nano. 2009;**3**:2274-2280. DOI: 10.1021/nn9002067

[87] Park EJ, Shim HW, Lee GH, Kim JH, Kim DW. Comparison of toxicity between the different-type TiO_2 nanowires *in vivo* and *in vitro*. Archives of Toxicology. 2013;**87**:1219-1230. DOI: 10.1007/s00204-013-1019-3

[88] Vallee BL, Falchuk KH. The biochemical basis of zinc physiology. Physiological Reviews. 1993;**73**:79-105. DOI: 10.1152/physrev.1993.73.1.79

[89] Shankar AH, Prasad AS. Zinc and immune function: The biological basis of altered resistance to infection. American Journal of Clinical Nutrition. 1998;**68**:447S-463S

[90] Zhou J, Xu N, Wang ZL. Dissolving behavior and stability of ZnO wires in biofluids: A study on biodegradability and biocompatibility of ZnO nanostructures. Advanced Materials. 2006;**18**:2432-2435. DOI: 10.1002/adma.200600200

[91] Wang ZL. Zinc oxide nanostructures: Growth, properties and applications. Journal of Physics. Condensed Matter. 2004;**16**:R829-R858. DOI: 10.1088/0953-8984/16/25/R01

[92] Hanley C, Layne J, Punnoose A, Reddy KM, Coombs I, Coombs A, Feris K, Wingett D. Preferential killing of cancer cells and activated human T cells using ZnO nanoparticles. Nanotechnology. 2008;**19**:295103. DOI: 10.1088/0957-4484/19/29/295103

[93] Javed Akhtar M, Ahamed M, Kumar S, Majeed Khan M, Ahmad J, Alrokayan SA. Zinc oxide nanoparticles selectively induce apoptosis in human cancer cells through reactive oxygen species. International Journal of Nanomedicine. 2012;**7**:845-857. DOI: 10.2147/IJN.S29129

[94] Zhang H, Chen B, Jiang H, Wang C, Wang H, Wang X. A strategy for ZnO nanorod mediated multi-mode cancer treatment. Biomaterials. 2011;**32**:1906-1914. DOI: 10.1016/j.biomaterials.2010.11.027

[95] Mitra S, Subia B, Patra P, Chandra S, Debnath N, Das S, Banerjee R, Kundu SC, Pramanik P, Goswami A. Porous ZnO nanorod for targeted delivery of doxorubicin: in vitro and *in vivo* response for therapeutic applications. Journal of Materials Chemistry. 2012;**22**:24145-24154. DOI: 10.1039/C2JM35013K

[96] Hong H, Shi J, Yang Y, Zhang Y, Engle JW, Nickles RJ, Wang X, Cai W. Cancer-targeted optical imaging with fluorescent zinc oxide nanowires. Nano Letters. 2011;**11**:3744-3750. DOI: 10.1021/nl201782m

[97] Peulon S, Lincot D. Mechanistic study of cathodic electrodeposition of zinc oxide and zinc hydroxychloride films from oxygenated aqueous zinc chloride solutions. Journal of the Electrochemical Society. 1998;**145**:864-874. DOI: 10.1149/1.1838359

[98] Franklin NM, Rogers NJ, Apte SC, Batley GE, Gadd GE, Casey PS. Comparative toxicity of nanoparticulate ZnO, bulk ZnO, and $ZnCl_2$ to a freshwater microalga (*Pseudokirchneriella subcapitata*): The importance of particle solubility. Environmental Science & Technology. 2007;**41**:8484-8490. DOI: 10.1021/es071445r

[99] Xia T, Kovochich M, Liong M, Mädler L, Gilbert B, Shi H, Yeh JI, Zink JI, Nel AE. Comparison of the mechanism of toxicity of zinc oxide and cerium oxide nanoparticles based on dissolution and oxidative stress properties. ACS Nano. 2008;**2**:2121-2134. DOI: 10.1021/nn800511k

[100] Vandebriel RJ, De Jong WH. A review of mammalian toxicity of ZnO nanoparticles. Nanotechnology, Science and Applications. 2012;**5**:61-71. DOI: 10.2147/NSA.S23932

[101] Reddy KM, Feris K, Bell J, Wingett DG, Hanley C, Punnoose A. Selective toxicity of zinc oxide nanoparticles to prokaryotic and eukaryotic systems. Applied Physics Letters. 2007;**90**:213902-1–213902-3. DOI: 10.1063/1.2742324

[102] Hanley C, Thurber A, Hanna C, Punnoose A, Zhang J, Wingett DG. The influences of cell type and ZnO nanoparticle size on immune cell cytotoxicity and cytokine induction. Nanoscale Research Letters. 2009;**4**:1409-1420. DOI: 10.1007/s11671-009-9413-8

[103] Deng X, Luan Q, Chen W, Wang Y, Wu M, Zhang H, Jiao Z. Nanosized zinc oxide particles induce neural stem cell apoptosis. Nanotechnology. 2009;**20**:115101. DOI: 10.1088/0957-4484/20/11/115101

[104] Premanathan M, Karthikeyan K, Jeyasubramanian K, Manivannan G. Selective toxicity of ZnO nanoparticles toward Gram-positive bacteria and cancer cells by apoptosis through lipid peroxidation. Nanomedicine: Nanotechnology, Biology and Medicine. 2011;**7**:184-192. DOI: 10.1016/j.nano.2010.10.001

[105] Lane DP. Cancer p53, guardian of the genome. Nature. 1992;**358**:15-16. DOI: 10.1038/358015a0

[106] Ng KW, Khoo SPK, Heng BC, Setyawati MI, Tan EC, Zhao XX, Xiong SJ, Fang WR, Leong DT, Loo JSC. The role of the tumor suppressor p53 pathway in the cellular DNA damage response to zinc oxide nanoparticles. Biomaterials. 2011;**32**:8218-8225. DOI: 10.1016/j.biomaterials.2011.07.036

[107] Sharma V, Anderson D, Dhawan A. Zinc oxide nanoparticles induce oxidative DNA damage and ROS-triggered mitochondria mediated apoptosis in human liver cells (HepG2). Apoptosis. 2012;**17**:852-870. DOI: 10.1007/s10495-012-0705-6

[108] Kao YY, Chiung YM, Chen YC, Cheng TJ, Liu PS. Zinc oxide nanoparticles interfere with zinc ion homeostasis to cause cytotoxicity. Toxicological Sciences. 2012;**125**:462-472. DOI: 10.1093/toxsci/kfr319

[109] Othman BA, Greenwood C, Abuelela AF, Bharath AA, Chen S, Theodorou I, Douglas T, Uchida M, Ryan M, Merzaban JS, Porter AE. Correlative light-electron microscopy shows RGD-targeted ZnO nanoparticles dissolve in the intracellular environment of triple negative breast cancer cells and cause apoptosis with intratumor heterogeneity. Advanced Healthcare Materials. 2016;**5**:1310-1325. DOI: 10.1002/adhm.201501012

[110] Li Z, Yang R, Yu M, Bai F, Li C, Wang ZL. Cellular level biocompatibility and biosafety of ZnO nanowires. Journal of Physical Chemistry C. 2008;**112**:20114-20117. DOI: 10.1021/jp808878p

[111] Müller KH, Kulkarni J, Motskin M, Goode A, Winship P, Skepper JN, Ryan MP, Porter AE. pH-dependent toxicity of high aspect ratio ZnO nanowires in macrophages due to intracellular dissolution. ACS Nano. 2010;**4**:6767-6779. DOI: 10.1021/nn101192z

[112] Gong C, Tao G, Yang L, Liu J, He H, Zhuang Z. The role of reactive oxygen species in silicon dioxide nanoparticle-induced cytotoxicity and DNA damage in HaCaT cells. Molecular Biology Reports. 2012;**39**:4915-4925. DOI: 10.1007/s11033-011-1287-z

[113] Huan C, Shu-Qing S. Silicon nanoparticles: Preparation, properties, and applications. Chinese Physics B. 2014;**23**:88102. DOI: 10.1088/1674-1056/23/8/088102

[114] Xing X, He X, Peng J, Wang K, Tan W. Uptake of silica-coated nanoparticles by HeLa cells. Journal of Nanoscience and Nanotechnology. 2005;**5**:1688-1693. DOI: 10.1166/jnn.2005.199

[115] Yan L, Wang H, Zhang A, Zhao C, Chen Y, Li X. Bright and stable near-infrared pluronic–silica nanoparticles as contrast agents for *in vivo* optical imaging. Journal of Materials Chemistry B. 2016;**4**:5560-5566. DOI: 10.1039/C6TB01234E

[116] Bahadar H, Maqbool F, Niaz K, Abdollahi M. Toxicity of nanoparticles and an overview of current experimental models. Iranian Biomedical Journal. 2016;**20**:1. DOI: 10.7508/ibj.2016.01.001

[117] Lin W, Huang Y, Zhou X-D, Ma Y. *In vitro* toxicity of silica nanoparticles in human lung cancer cells. Toxicology and Applied Pharmacology. 2006;**217**:252-259. DOI: 10.1016/j.taap.2006.10.004

[118] Li Y, Sun L, Jin M, Du Z, Liu X, Guo C, Li Y, Huang P, Sun Z. Size-dependent cytotoxicity of amorphous silica nanoparticles in human hepatoma HepG2 cells. Toxicology in Vitro. 2011;**25**:1343-1352. DOI: 10.1016/j.tiv.2011.05.003

[119] Sahu D, Kannan GM, Tailang M, Vijayaraghavan R. *In vitro* cytotoxicity of nanoparticles: A comparison between particle size and cell type. Journal of Nanoscience. 2016;**2016**. DOI: 10.1155/2016/4023852

[120] Zhu J, Liao L, Zhu L, Zhang P, Guo K, Kong J, Ji C, Liu B. Size -dependent cellular uptake efficiency, mechanism, and cytotoxicity of silica nanoparticles toward HeLa cells. Talanta. 2013;**107**:408-415. DOI: 10.1016/j.talanta.2013.01.037

[121] Lu X, Qian J, Zhou H, Gan Q, Tang W, Lu J, Yuan Y, Liu C. *In vitro* cytotoxicity and induction of apoptosis by silica nanoparticles in human HepG2 hepatoma cells. International Journal of Nanomedicine. 2011;**6**:1889-1901. DOI: 10.2147/IJN.S24005

[122] Ahmad J, Ahamed M, Akhtar MJ, Alrokayan SA, Siddiqui MA, Musarrat J, Al-Khedhairy AA. Apoptosis induction by silica nanoparticles mediated through reactive oxygen species in human liver cell line HepG2. Toxicology and Applied Pharmacology. 2012;**259**:160-168. DOI: 10.1016/j.taap.2011.12.020

[123] Kim I-Y, Joachim E, Choi H, Kim K. Toxicity of silica nanoparticles depends on size, dose, and cell type. Nanomedicine: Nanotechnology, Biology and Medicine. 2015;**11**:1407-1416. DOI: 10.1016/j.nano.2015.03.004

[124] Bhattacharjee S, Rietjens IMCM, Singh MP, Atkins TM, Purkait TK, Xu Z, Regli S, Shukaliak A, Clark RJ, Mitchell BS, Alink GM, Marcelis ATM, Fink MJ, Veinot JGC, Kauzlarich SM, Zuilhof H. Cytotoxicity of surface-functionalized silicon and germanium nanoparticles: The dominant role of surface charges. Nanoscale. 2013;**5**:4870. DOI: 10.1039/c3nr34266b

[125] Park Y-H, Bae HC, Jang Y, Jeong SH, Lee HN, Ryu W-I, Yoo MG, Kim Y-R, Kim M-K, Lee JK. Effect of the size and surface charge of silica nanoparticles on cutaneous toxicity. Molecular & Cellular Toxicology. 2013;**9**:67-74. DOI: 10.1007/s13273-013-0010-7

[126] Julien DC, Richardson CC, Beaux MF, McIlroy DN, Hill RA. *in vitro* proliferating cell models to study cytotoxicity of silica nanowires. Nanomedicine: Nanotechnology, Biology and Medicine. 2010;**6**:84-92. DOI: 10.1016/j.nano.2009.03.003

[127] Peng F, Su Y, Wei X, Lu Y, Zhou Y, Zhong Y, Lee S, He Y. Silicon-nanowire-based nanocarriers with ultrahigh drug-loading capacity for in vitro and *in vivo* cancer therapy. Angewandte Chemie, International Edition. 2013;**52**:1457-1461. DOI: 10.1002/anie.201206737

[128] Salata OV. Applications of nanoparticles in biology and medicine. Journal of Nanobiotechnology. 2004;**2**:3. DOI: 10.1186/1477-3155-2-3

[129] Adili A, Crowe S, Beaux MF, Cantrell T, Shapiro PJ, McIlroy DN, Gustin KE. Differential cytotoxicity exhibited by silica nanowires and nanoparticles. Nanotoxicology. 2008;**2**:1-8. DOI: 10.1080/17435390701843769

[130] Zhang W, Tong L, Yang C. Cellular binding and internalization of functionalized silicon nanowires. Nano Letters. 2012;**12**:1002-1006. DOI: 10.1021/nl204131n

[131] Barroso MM. Quantum dots in cell biology. Journal of Histochemistry and Cytochemistry. 2011;**59**:237-251. DOI: 10.1369/0022155411398487

[132] Kairdolf BA, Smith AM, Stokes TH, Wang MD, Young AN, Nie S. Semiconductor quantum dots for bioimaging and biodiagnostic applications. Annual Review of Analytical Chemistry. 2013;**6**:143-162. DOI: 10.1146/annurev-anchem-060908-155136

[133] Du Y, Guo S. Chemically doped fluorescent carbon and graphene quantum dots for bioimaging, sensor, catalytic and photoelectronic applications. Nanoscale. 2016;**8**:2532-2543. DOI: 10.1039/C5NR07579C

[134] Luo PG, Sahu S, Yang S-T, Sonkar SK, Wang J, Wang H, LeCroy GE, Cao L, Sun Y-P. Carbon "quantum" dots for optical bioimaging. Journal of Materials Chemistry B. 2013; **1**:2116-2127. DOI: 10.1039/C3TB00018D

[135] Qian Z, Shan X, Chai L, Ma J, Chen J, Feng H. Si-doped carbon quantum dots: A facile and general preparation strategy, bioimaging application, and multifunctional sensor. ACS Applied Materials & Interfaces. 2014;**6**:6797-6805. DOI: 10.1021/am500403n

[136] Wegner KD, Hildebrandt N. Quantum dots: Bright and versatile *in vitro* and *in vivo* fluorescence imaging biosensors. Chemical Society Reviews. 2015;**44**:4792-4834. DOI: 10.1039/C4CS00532E

[137] Zhang J, Ma Y, Li N, Zhu J, Zhang T, Zhang W, Liu B. Preparation of graphene quantum dots and their application in cell imaging. Journal of Nanomaterials. 2016;**2016**. DOI: 10.3109/21691401.2015.1052468

[138] Bajwa N, Mehra NK, Jain K, Jain NK. Pharmaceutical and biomedical applications of quantum dots. Artificial Cells, Nanomedicine, Biotechnology. 2016;**44**:758-768. DOI: 10.3109/21691401.2015.1052468

[139] Zhou J, Yang Y, Zhang C. Toward biocompatible semiconductor quantum dots: From biosynthesis and bioconjugation to biomedical application. Chemical Reviews. 2015;**115**:11669-11717. DOI: 10.1021/acs.chemrev.5b00049

[140] Tsoi KM, Dai Q, Alman BA, Chan WCW. Are quantum dots toxic? Exploring the discrepancy between cell culture and animal studies. Accounts of Chemical Research. 2012;**46**:662-671

[141] Yong KT, Law W-C, Hu R, Ye L, Liu L, Swihart MT, Prasad PN. Nanotoxicity assessment of quantum dots: From cellular to primate studies. Chemical Society Reviews. 2013;**42**:1236-1250. DOI: 10.1039/C2CS35392J

[142] Derfus AM, Chan WCW, Bhatia SN. Probing the cytotoxicity of semiconductor quantum dots. Nano Letters. 2004;**4**:11-18. DOI: 10.1039/C2CS35392J

[143] Godt J, Scheidig F, Grosse-Siestrup C, Esche V, Brandenburg P, Reich A, Groneberg DA. The toxicity of cadmium and resulting hazards for human health. Journal of Occupational Medicine and Toxicology. 2006;**1**:21-22, 2006. DOI: 10.1186/1745-6673-1-22

[144] Fellahi O, Sarma RK, Das MR, Saikia R, Marcon L, Coffinier Y, Hadjersi T, Maamache M, Boukherroub R. The antimicrobial effect of silicon nanowires decorated with silver and copper nanoparticles. Nanotechnology. 2013;24. DOI: 10.1088/0957-4484/24/49/495101

[145] Chen N, He Y, Su Y, Li X, Huang Q, Wang H, Zhang X, Tai R, Fan C. The cytotoxicity of cadmium-based quantum dots. Biomaterials. 2012;**33**:1238-1244. DOI: 10.1016/j.biomaterials.2011.10.070

[146] Soenen SJ, Manshian BB, Aubert T, Himmelreich U, Demeester J, De Smedt SC, Hens Z, and Braeckmans K. Cytotoxicity of cadmium-free quantum dots and their use in cell bioimaging. Chemical Research in Toxicology. 2014;**27**:1050-1059. DOI: 10.1021/tx5000975

[147] Dinan NM, Atyabi F, Rouini M-R, Amini M, Golabchifar A-A, Dinarvand R. Doxorubicin loaded folate-targeted carbon nanotubes: Preparation, cellular internalization, in vitro cytotoxicity and disposition kinetic study in the isolated perfused rat liver. Materials Science and Engineering. 2014;**39**:47-55. DOI: http://dx.doi.org/10.1016/j.msec.2014.01.055

IntechOpen